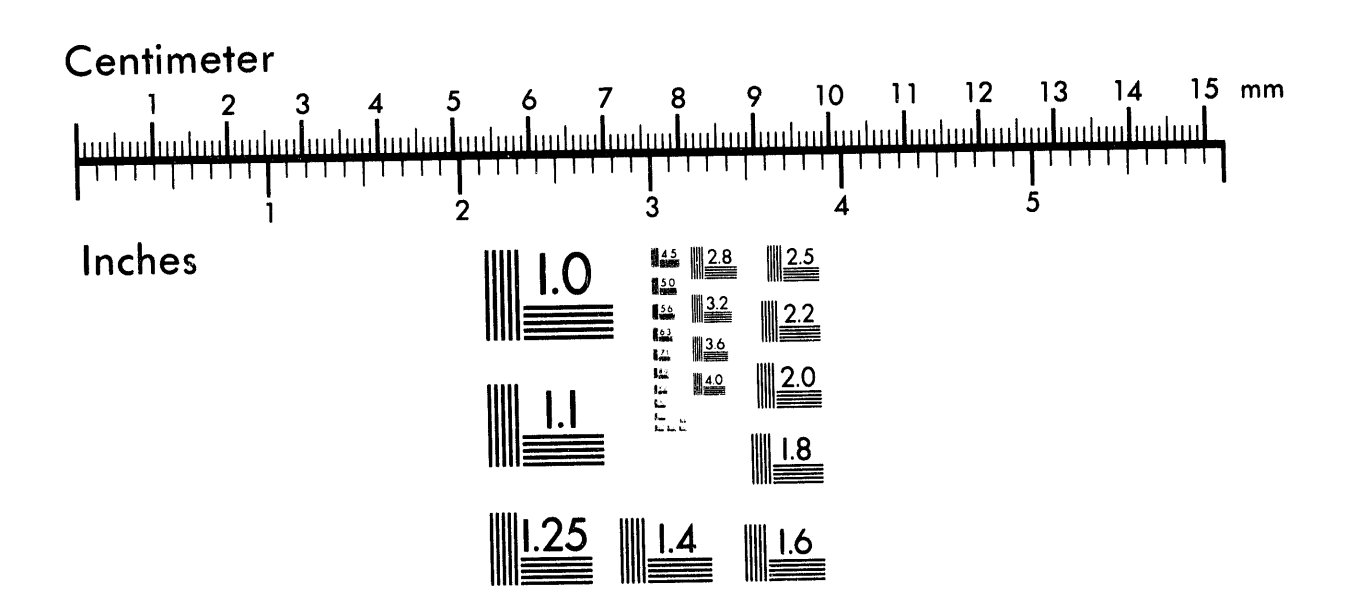
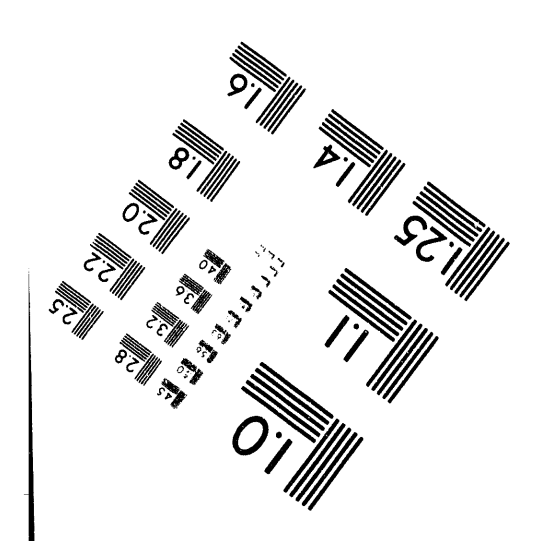




Association for Information and Image Management

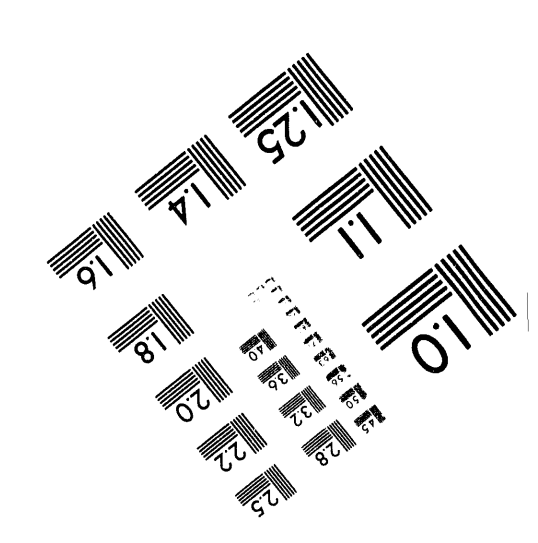
1100 Wayne Avenue, Suite 1100 Silver Spring, Maryland 20910 301/587-8202



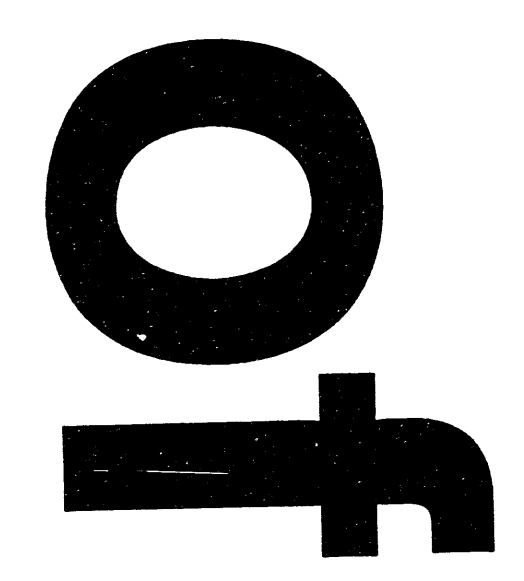


MANUFACTURED TO AIIM STANDARDS

BY APPLIED IMAGE, INC.









ANTIPROTON PRODUCTION IN CENTRAL Si+Au COLLISIONS AT 14.6 A.GeV/c

Peter J. Rothschild Laboratory for Nuclear Science and Physics Department Massachusetts Institute of Technology, Cambridge, MA 02139, USA

for Experiment E859 (E802 Collaboration): ANL-BNL-UCBerkelev-UCRiverside-Columbia-Hiroshima-INS-Kyushu-LLNL-MIT-NYU-Tokyo-Tsukuba

ABSTRACT

Antiproton measurements made by E802 have been extended to lower rapidities, while in those y-pT regions already studied the statistics have been improved by approximately an order of magnitude. We present the dn/dy distribution for antiproton production in central 14.6 A.GeV/c Si+Au collisions in the rapidity range 0.8 < y < 1.8. In addition, antilambda production has been detected for the first time in these collisions at the AGS.

1. Introduction

At the AGS momentum of 14.6 A.GeV/c, central collisions of Si+Au are believed to be in the "stopping" regime, where the projectile nucleus is essentially stopped by the target nucleus in the center-of-mass system. Much of the kinetic energy of the projectile is then transferred into compressing and heating the target/projectile system, and very high baryon densities, on the order of 3-5 times ordinary nuclear density, are believed to be reached. Under such extreme conditions, it has been predicted that ordinary hadronic matter undergoes a phase transition to the quark matter phase. One of the predicted signatures of quark matter formation is the enhanced production of antibaryons.

Regardless of whether or not the critical energy density to produce quark matter is reached at the AGS, the large annihilation cross section for antiprotons makes a very useful probe of the baryon density reached in these collisions. The annihilation also makes the antiproton yield sensitive to the formation time of the antiproton. If the formation time is large, most of the antiprotons will be fully formed only after they have passed through the surrounding baryon-rich collision region, and will not be absorbed. If, on the other hand, the formation time is short (of the order of 1 fm/c), many of the antiprotons will be absorbed, reducing the yield.

Experiment E859 is an extension of E802, using additional tracking chambers and a new second level trigger to provide on-line particle identification. This trigger has the ability to select particles based on mass and charge, making it possible to study rare particles, such as antiprotons, with greatly enhanced statistics. E802 reconstructed and identified approximately 1,000 antiprotons in the rapidity range 0.9 < y < 1.7 and in the transverse

> MASTER endings from of the document by the

momentum range $0.3 < p_T < 1.2 \ GeV/c$, for two targets. Using the on-line trigger experiment E859 has more than 10,000 events containing an antiproton. These data extend the range of the E802 measurement in both rapidity and transverse momentum, and provide much greater accuracy in the parameterization of distributions.

With existing E802 data, the ability to determine the antiproton inverse slopes was severely limited by low statistics. For antiprotons produced in Si+A collisions, it was found that the inverse slopes have an average value of 140 MeV with experimental uncertainties of between 20 and 40 MeV. Within these uncertainties it was found that the inverse slopes are independent of target and collision centrality. Using the E859 data we have been able to measure the antiproton inverse slopes to within an uncertainty of 15 MeV for several rapidity intervals. Such data will hopefully determine the (presently poorly-understood) relative rates of production and re-absorption of antiprotons.

2. Results

Antiproton data were collected at the 5, 14 and 24 degree spectrometer settings (with some low statistics data at 34 and 44 degrees) for Si on Au and Al targets. During the dedicated antiproton running periods, the spectrometer was only triggered by events containing a negatively charged particle with a mass greater than 0.7 GeV/c^2 . This configuration increased the antiproton trigger rate by a factor of between 20 and 50. Many of the antiprotons, however, were collected using trigger configurations that looked for the "or" of an antiproton and either a K^- or a pair of K^+ 's.

Approximately one half of the central Si+Au antiproton data set from E859 has been analyzed, including all of the 5 degree data and half of the 14 and 24 degree data. The data analyzed cover the transverse momentum range $0.25 < p_T < 1.80$ GeV/c and the rapidity range 0.8 < y < 1.8.

The measured mass distribution in the antiproton region from the combined data are shown in Fig. 1. The antiprotons were selected by calculating δTOF , the difference between the measured time-of-flight and the expected value of the time-of-flight, assuming the particle was an antiproton. The width of this distribution was measured using protons in several momentum slices, and the width was parameterized as a function of momentum. An antiproton at a given momentum was then required to have a δTOF within the 3σ limits of the distribution for that momentum.

Central collisions were defined by a cut on the observed charged particle multiplicity corresponding to the upper 7% of the distribution.

The invariant differential yield as a function of transverse mass (m_T) is shown in Fig. 2 for four different rapidity slices for the data that have been analyzed. The transverse mass is defined by $m_T = \sqrt{m_p^2 + p_T^2}$, where m_p is the proton mass. The yields were fitted with a two-parameter exponential function in m_T of the form

$$E\frac{d^3n}{dp^3} = \frac{1}{2\pi m_T} \frac{d^2n}{dm_T dy} = \frac{1}{2\pi} \frac{e^{(m_p/T)}}{T(m_p + T)} \cdot \frac{dn}{dy} \cdot e^{-(m_T/T)}.$$

The free parameters in the fit are T (the inverse m_T slope or temperature) and dn/dy. The inverse m_T slopes of these fits are shown in Fig. 3 for each rapidity slice. The error bars on

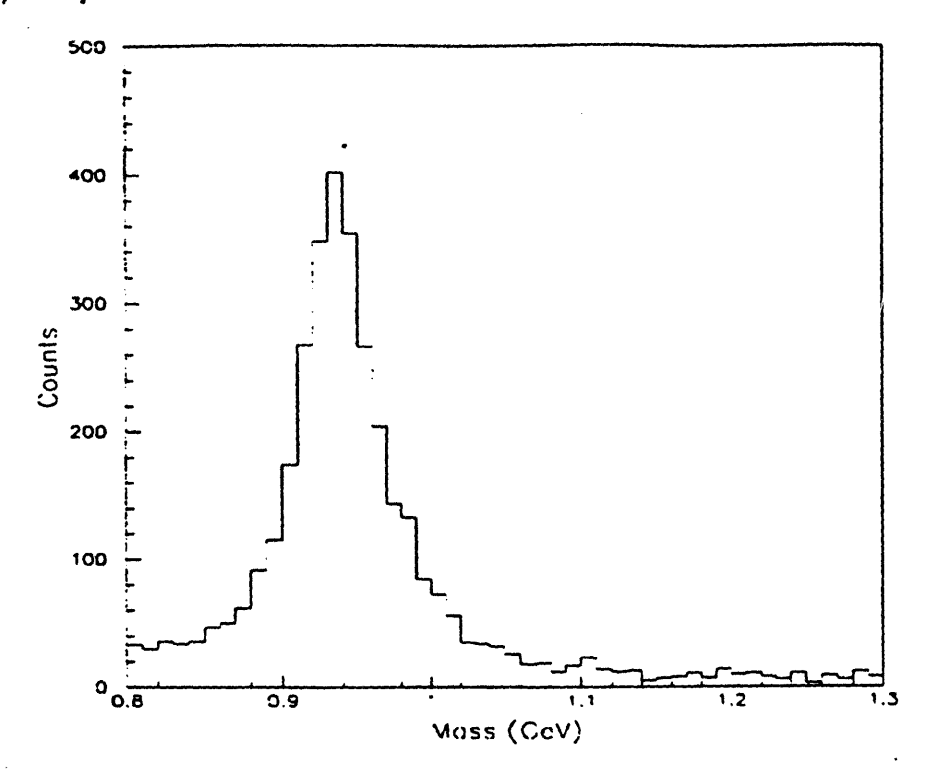


Fig. 1: Measured mass distribution in the antiproton mass region.

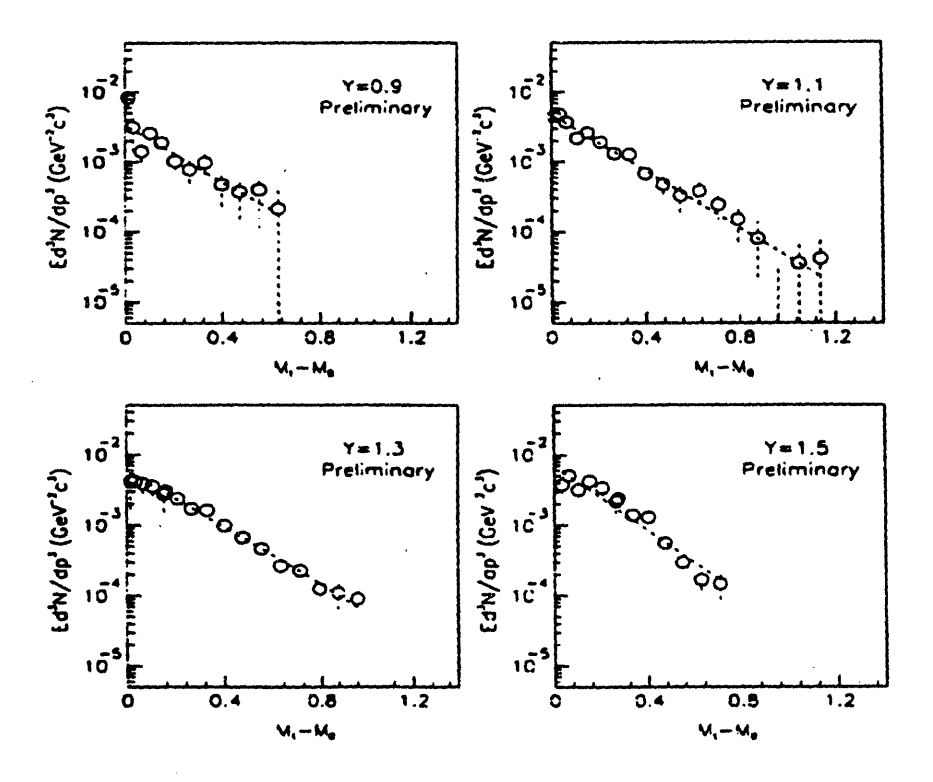


Fig. 2: Preliminary invariant m_T spectra for antiprotons in central Si+Au collisions for four rapidity slices ($\delta y = 0.2$).

the state of the state of the state of

I

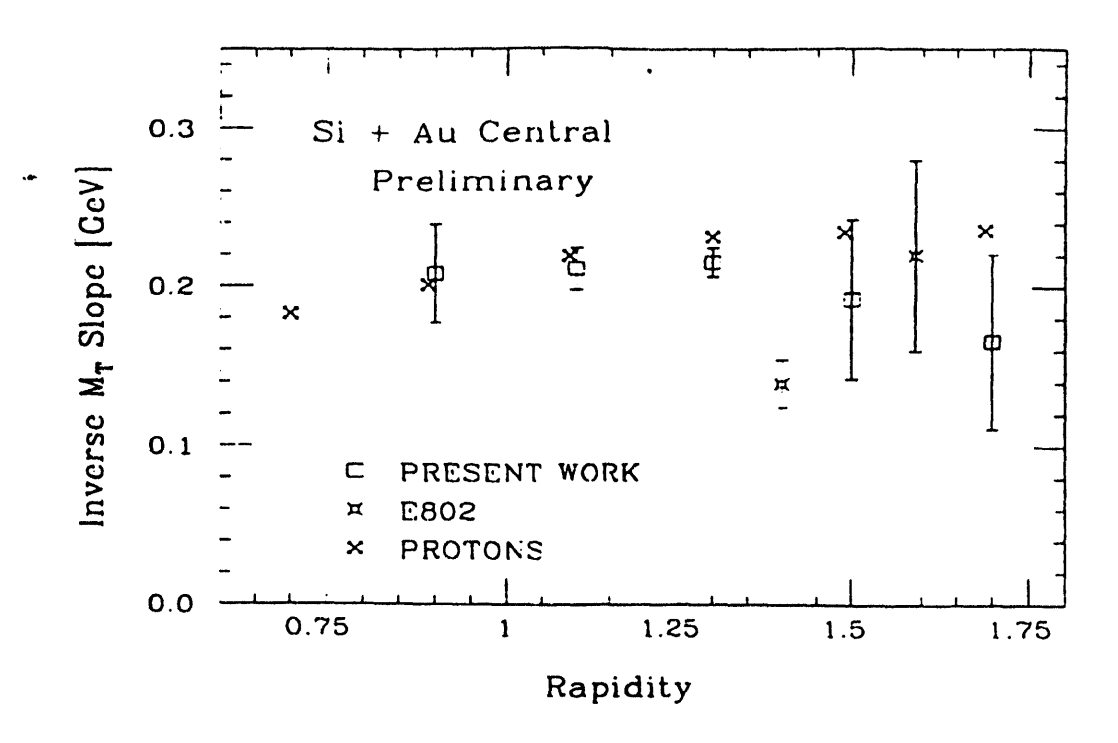


Fig. 3: Inverse m_T slopes for antiprotons in central Si+Au collisions. The inverse slopes for protons from E802 are shown for comparison.

these measurements are purely statistical, and should decrease once all the data are merged and the yields can be fitted over a larger range of m_T.

The dn/dy values obtained from the fits are shown in Fig. 4. The corrections applied to the data for track reconstruction inefficiency and antiproton annihilation in the target and spectrometer were momentum dependent, and were between 9% and 38%, with the mean correction being 11%. The data were also corrected for the residual background below the antiproton peak. The identification of antiprotons was reasonably clean for the 14 and 24 degree spectrometer settings, where the background is approximately 10%, but the background is considerably larger for the 5 degree data (approximately 38%). Each of the corrections is known to an accuracy of about 5%.

It can be seen in Fig. 4 that the dn/dy distribution lies below that measured in E802 for rapidities above y=1.2, but the statistical errors on the E802 data are large. From Fig. 3 the inverse m_T slopes are fairly constant with rapidity at a mean value of approximately 213 ± 15 MeV, and apparently drop off slightly above y=1.3. The two data points from E802 are taken from the thesis of J. Costales.² In particular, the slope of 135 ± 20 MeV found by E802 at y=1.4 is well below the E859 value of 204 ± 8 MeV at that rapidity. From these preliminary results, it appears that the inverse m_T slopes are similar for protons and antiprotons, at least for rapidities below y=1.3. Such similarity is consistent with the prediction of hydrodynamical expansion models.³

In Fig. 5 the invariant m_T spectrum for the rapidity slice y=1.6 is shown with the measurements from experiments E858⁴ and E814⁵ near $m_T=0$ (low p_T). It can be seen that the exponential m_T extrapolation through the E859 data appears to overpredict the yield

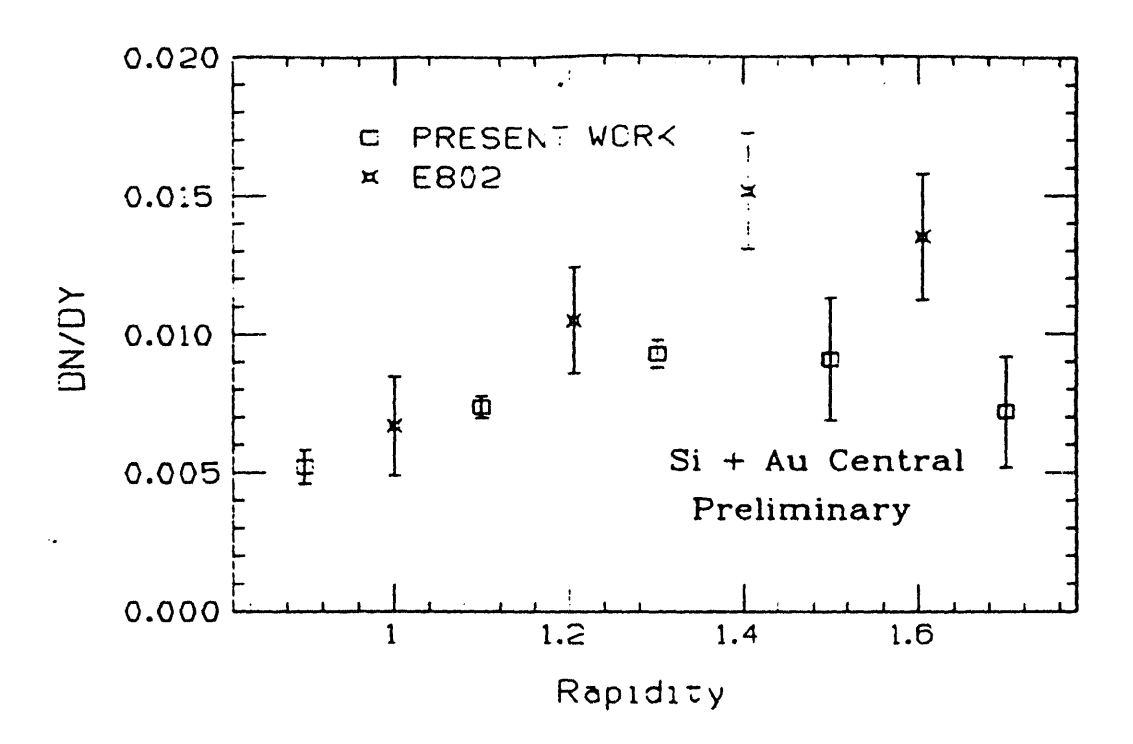


Fig. 4: Rapidity density distribution for antiprotons in central Si+Au collisions.

 $m_T=0$, although it could also be said that the E859 and E814 measurements are consistent with one another within the statistical errors. It should be noted that the E859 data is selected on central events while the other two are not (see the contribution by Crawford for more discussion of this point). Another possible explanation for a discrepancy is that the lower momentum (low m_T) component is being absorbed. However, this effect should then be even more conspicuous for the antiprotons with low momentum relative to the spectator target material, and curvature at low m_T should be more pronounced in the spectra as we approach the target rapidity at y=0. This is not seen in the E859 data, which are similarly well described by exponentials in m_T at low rapidity (see Fig. 2).

The invariant mass spectrum of antiproton- π^+ pairs from the data taken at the 14 degree spectrometer setting is shown in Fig. 6. The presence of the peak at the mass of the antilambda ($m_{inv} = 1.116 \text{ GeV/c}^2$), after the background has been subtracted, indicates that some of the detected antiprotons are from the antilambda decay channel. The measured antilambda yield was 38±6. The background was calculated by finding the invariant mass distribution of π^+ 's and antiprotons taken from different events, and then scaling it until it matched the real invariant mass distribution on either side of the antilambda peak.

The acceptance calculation for the detection and reconstruction of antilambdas in the E859 spectrometer has not been completed. However, by taking the ratio of the antilambda yield to the lambda yield measured by E859 at the opposite magnet polarity⁶ the acceptance factors cancel one another. For central Si+Au collisions we measure the ratio $\overline{\Lambda}/\Lambda = 0.0023 \pm 0.0008$ at a mean rapidity of 1.4.

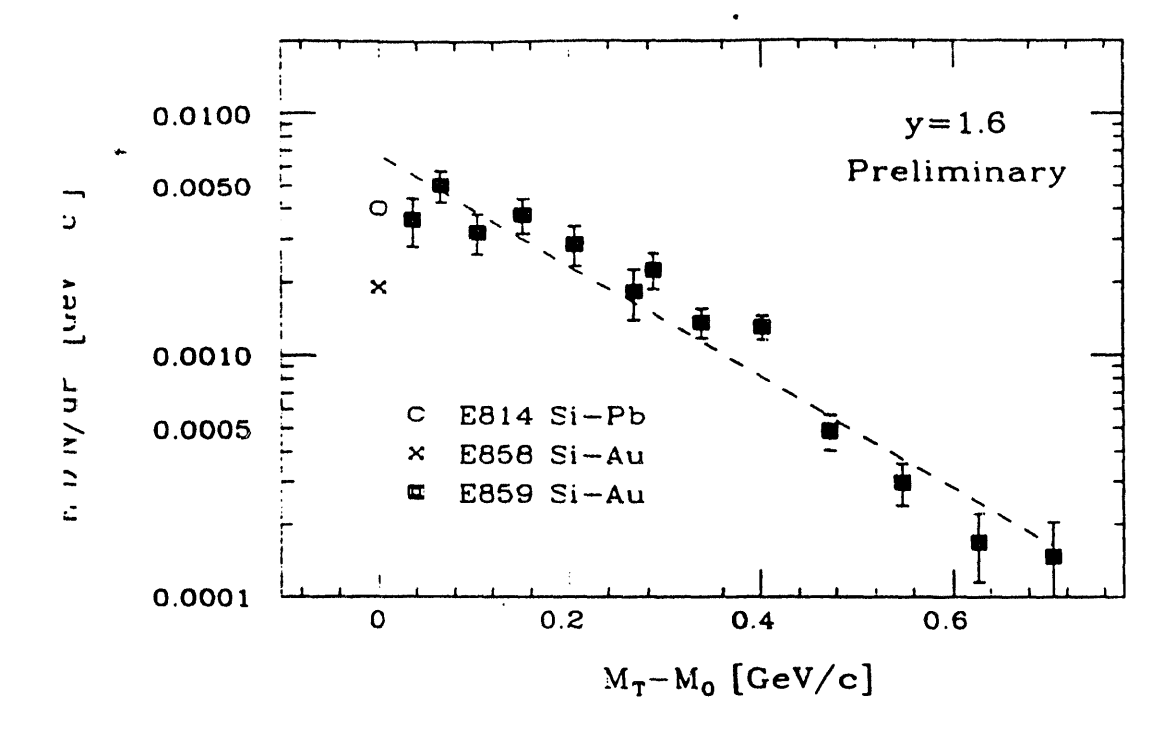


Fig. 5: Preliminary invariant m_T spectrum for antiprotons in central Si+Au collisions for the y=1.6 rapidity slice ($\delta y = 0.4$).

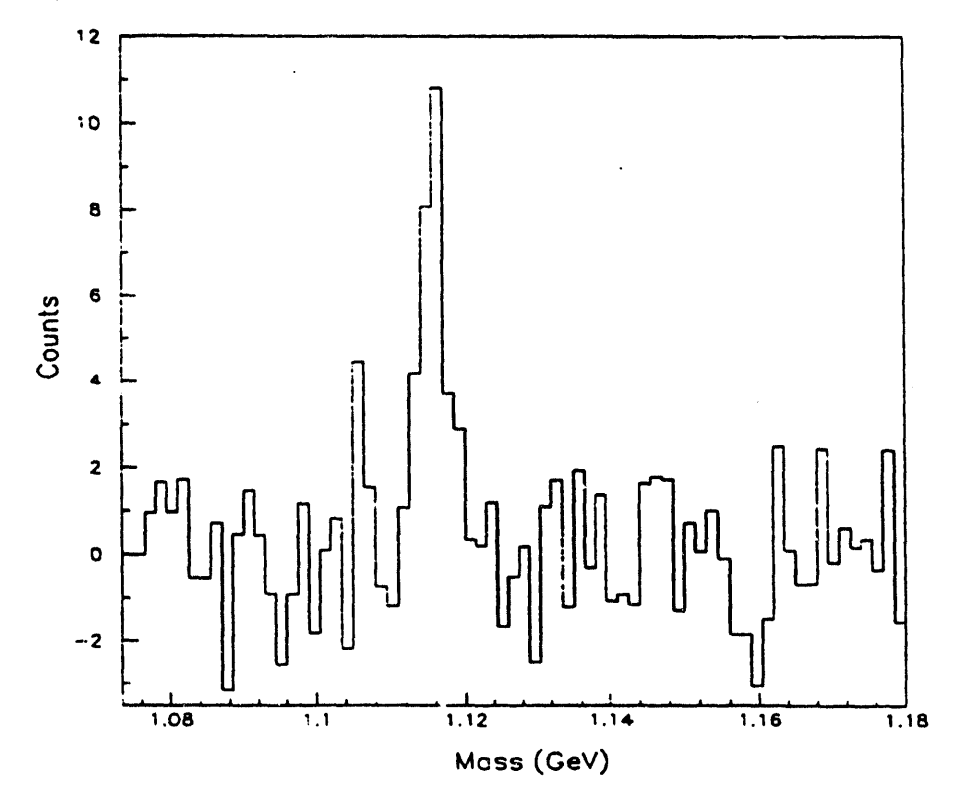


Fig. 6: Invariant mass spectrum of antiproton and π^+ pairs in central Si+Au collisions, with the background subtracted. The antilambda peak can be seen at 1.116 GeV/c².

10.

t

r d 2 n

re ti or

w; .ex

4.

E8

B.

COI

3. Model Comparisons and Conclusion

The antiproton yield measured in E859 is essentially what one would expect if it is assumed that the antiprotons all come from the first nucleon-nucleon collisions, and that there is no subsequent absorption of the antiprotons. If there is large absorption, however, it is clear that there must be a corresponding enhancement of the initial antiproton production.

This is the picture that emerges from the RQMD model, which produces an antiproton yield in Si+Al that is 3-4 times higher than expected from the simple first collision model. The mechanism for this is a collective process in which baryons which are below the antiproton production threshold after their first collision are excited to high-lying resonances in subsequent collisions. The resonances then decay into antibaryons. This enhanced production however, is offset in RQMD by a high probability of absorption, which is strongly dependent on the system mass. For Si+Al collisions only 35% of the antiprotons survive, while for Si+Au collisions the probability is down to 15%. With the enhanced production and large annihilation rates RQMD is able to reproduce the E802 measured yield reasonably well.

The antiproton yields predicted by the ARC code. "A Relativistic Cascade", also agree well with the E802 results. For Si+Au, however, almost all the antiprotons in ARC come from the first high-energy baryon-baryon collisions, resulting in a lower primary production rate than in RQMD. The amount of absorption, without any screening effects, is similar to that in RQMD. The ARC model, however, includes a three-body screening effect that dramatically reduces the amount of antiproton absorption, allowing 66% of the antiprotons to survive in Si+Au collisions. To summarize, the reduced primary production rate of antiprotons in ARC relative to RQMD is compensated by the screening effect, which greatly reduces the effects of absorption.

The E859 high-statistics measurement of the inverse slopes of the m_T spectra for various rapidity slices also provides a means for comparing the models with the data. ARC predicts an average value of 170 ± 20 MeV, in reasonable agreement with the average value of 207 ± 20 MeV measured in E859 over the rapidity range 1.1 < y < 1.7. Inverse slopes are not yet available for RQMD.

The ability to discriminate between the two pictures of production and re-absorption represented in ARC and RQMD will depend on a systematic, high-statistics study of antiproton production in different collision systems. The discussion should become clearer once the Si+Al data from E859 are analyzed. A definitive statement, however, may have to wait until antiproton data are available from the Au+Au collisions which will be studied by experiment E866.

4. Acknowledgements

Special thanks are due to Craig Ogilvie for helping me pull this talk together. Experiment E859 is supported in part by the U.S. Department of Energy contracts and grants with ANL, BNL, UC-Berkeley, UC-Riverside, Columbia. LLNL, and MIT, in part by NASA under contract with UC-Berkeley and by the US-Japan High Energy Physics Collaboration treaty.

5. References

- 1. T. Abbott et al., Phys. Lett. B271, 447 (1991)
- 2. J. Costales. Ph.D. Thesis. MIT (1990)
- 3. C.M. Ko and L. Xia, Phys. Rev. C38, 179 (1988) U. Heinz et al., Phys. Rev. C37, 1463 (1988)
- 4. P. Stankus et al., Nucl. Phys. A544, 603c (1992)
- 5. J.Barrette et al., Phys. Rev. Lett. 70, 1763 (1993)
- 6. T.W. Sung, Private Communication, MIT (1993)
- 7. A.Jahns, H.Stocker, W.Greiner and H.Sorge, Phys. Rev. Lett. 68, 2895 (1992)
- 8. S.H.Kahana, Y.Pang, T.Schlagel and C.B.Dover, Antiproton Production from Heavy Ion Collisions at 14.6 GeV/c, BNL preprint (1992)

DATE FILMED 6/29/94

İ		